Korean J. Chem. Eng., **29**(5), 555-562 (2012)
DOI: 10.1007/s11814-011-0230-2

JOURNAL REVIEW

Photodecomposition of polyphenols in *E. camaldulensis* leaves in the presence of hybrid catalyst of titania and MCM-41 synthesized from rice husk silica

Surachai Artkla†

Faculty of Art and Science, Roi-Et Rajabhat University, Selaphum, Roi-Et 45120, Thailand
(*Received 13 July 2011 • accepted 31 August 2011*)

Abstract–Photocatalytic degradation (PCD) of polyphenols (gallic acid) from *E. camaldulensis* leaves on TiO_2/MCM-41 was investigated in order to get rid of substances harmful to aquatic life. The TiO_2/MCM-41 catalysts with titania loading of 2-40% were synthesized by hydrothermal method using rice husk silica and tetraethyl orthotitanate as silica and titania sources, respectively. The obtained catalysts were characterized by XRD, TEM, Zeta potential analyzer, N_2 adsorption-desorption and diffuse reflectance UV spectroscopy. Hexagonal array of MCM-41 was confirmed, but its crystallinity decreased dramatically with titania loading. Zeta potential of TiO_2/MCM-41s surface varied from 2.11 to 6.00 with the increase of TiO_2 from 0 to 100 wt%. Band gap energy of TiO_2 shifted from 394.1 to 425.1 nm after adding 60%MCM-41 (40%TiO_2/MCM-41), facilitating the ease of OH establishment. Gallic acid - a weak acid solution (pK_a= 4.0) around 27 ppm was favorable to dissolve in water. PCD of gallic acid was carried out on irradiating of 400 W of mercury lamp. The results showed gallic acid solution about 10 wt% properly adsorbed on 10%TiO_2/MCM-41 and effectively degraded at pH solution of 9.0. PCD completed at 60 minutes of irradiation time through catalyst concentration of 0.17 g/L and obeyed pseudo-first order. Intermediate products were formic, oxalic, pyruvic, malanic and maleic acids that finally mineralized to CO_2 and H_2O as downstream products.

Key words: Eucalyptus, Polyphenols, Gallic Acid, MCM-41, Titania, Degradation

INTRODUCTION

Traditionally, *E. Camaldulensis* leaves containing complex polyphenolic substances were considered as anti-nutrients in animals because of the adverse effect of tannins (one type of polyphenols) on protein digestibility [1]. These complexes also show allelopathic effects, either reducing or ceasing the rate of germination of nearby natural and agricultural crops [2]. Gehrke et al. [3] investigated the effects of water-soluble polyphenols from *E. camaldulensis* litter in aquaria of golden perch (larvae of Macquaria ambigua). The golden perch was treated with a simulated annual litter density of 450 $g \cdot m^{-2}$ for 72 hours in a river red gum of *E. camaldulensis* litter. The results revealed that water became hypoxic with decreased pH and contained up to 30 mg/L tannin and lignin. Survival of 15-day-old and 8-day-old larvae was 14.9% and 0%, respectively, whereas a litter density of 1,223 $g \cdot m^{-2}$ resulted in total mortality for both age groups of larvae. Abelho and Graça [4] tested the hypothesis whether afforestation with *E. globulus* affected litter dynamics in streams and the structure of macroinvertebrate aquatic communities. The eucalyptus forest soils were highly hydrophobic, resulting in strong seasonal fluctuations in discharge. In autumn the communities of benthic macroinvertebrates of eucalyptus forest streams contained lower numbers of invertebrates than deciduous forest streams. Molina et al. [5] presented natural leachates of *E. globulus* (throughfall, stemflow and soil percolates) released toxic allelochemicals influencing the composition and structure of the understory of the plantation. The effect was mainly attributed to the decomposition products of decaying litter rather than to aerial leachates. Ahmed et al. [2] investigated allelopathic effects of different doses of *E. camaldulensis* leaf litter through five kinds of trees, including Falen (Vigna unguiculata), Chickpea (Cicer arietinum), Arhor (Cajanus cajan), Sada koroi (Albizia procera) and Ipil ipil (Leucaena leucocephala) at room temperature 27 °C with different doses of leaf litter extracts. The concentration of extract and litterfall of *E. camaldulesis* induced inhibitory effects. Higher concentration of the materials had the higher effect and vice versa.

As many negative effects of polyphenols in both aquatic lives and germination of plants, a number of processes are carried out to remove polyphenolic compounds. Biological processes do not work because phenolic compounds are major contributors to the toxicity and the antibacterial activity, which limits its microbial degradability [6]. Various kinds of pretreatments are required to moderate polyphenols prior to biological process. Most physical methods including precipitation, coagulation, filtration, flocculation/clarification and evaporation in open ponds only solve the problem partially [7]. Reverse osmosis, ultrafiltration and chemical treatment by ozone are usually expensive [8].

Advanced oxidation processes (AOPs) are useful methods for removing various kinds of organic compounds. Indeed, AOPs require the cooperation between TiO_2 and UV light to generate active species such as hydroxyl radical (•OH) and break down organic molecules via PCD. Such organic substrates, herbicides, pesticides, for instance, are able to degrade with these processes. Kim and Choi [9] studied PCD of tetramethylammonium (TMA) ion on bare TiO_2 at various pH solutions. The PCD on TiO_2 was effective in alkaline solution, but photoactivity of TiO_2 was lessened at pH 7 because of particle aggregation. Vohra et al. [10] impregnated bare TiO_2 particles with

†To whom correspondence should be addressed.
E-mail: surachaiartkla@yahoo.com

SiO_2 to modify the surface charge to a lower point of zero charge (pH_{PZC}) of titania. A hybrid catalyst of SiO_2-TiO_2 highly enhanced the PCD of TMA and prevented particle agglomeration of TiO_2 nanoparticles in a neutral solution. A complete conversion of TMA was achieved in 2 hours with SiO_2-TiO_2, whereas less than 80% conversion was obtained after 6 hours of irradiation with bare TiO_2 (at pH 5). Artkla et al. [11] dispersed TiO_2 Degussa P25 on MCM-41 synthesized from rice husk silica. The complete conversion of TMA was achieved in 90 minutes of irradiation at pH 7. The unsupported TiO_2 photocatalyst could convert only 20% of TMA in the same irradiation time and condition. According to the above explanation, this investigation aimed to modify the stability and surface properties of TiO_2 by adding MCM-41 to enhance the photodegradation of gallic acid in aqueous solution. Such circumstances including pH solution, irradiation time, adsorption aspect and kinetics of reaction were studied to elucidate PCD of this harmful solution.

EXPERIMENTAL SECTION

1. Chemicals and Methodology

Silica extraction method was adapted from a method described by Artkla et al. [12]. Chemicals for MCM-41 and TiO_2/MCM-41 synthesis were cetyltrimethylammonium bromide (CTABr, $C_{19}H_{42}BrN$, Ajax), sodium hydroxide (NaOH, Qrec), sulfuric acid (97% H_2SO_4, Qrec), hydrochloric acid (37% HCl, Qrec), tetrabutyl orthotitanate [$Ti(OC_4H_9)_4$, Fluka]. Chemicals for analysis of chemical compounds of *E. camaldulensis* leaves and PCD of polyphenols included lignin (Sigma), tannic acid (Sigma), gallic acid (sigma), flavone (Sigma). Apparatus for PCD were reaction bottle (pyrex reactor), needle (syringe) with nylon filter samples (PTFE), 0.45 μM in diameter and 400 W of UV lamp as the light source.

2. Preparation of MCM-41 and TiO_2/MCM-41s

MCM-41 was synthesized by mixing a molar ratio of 1.0SiO_2 : 3.0NaOH : 0.25CTABr : 180 H_2O in a Teflon-lined autoclave. Solution pH of the mixture was sequentially adjusted to 11.5 and a milky sol-gel was obtained. The gel mixture was crystallized at 100 °C for 72 hours. A solid-white powder of as-synthesized MCM-41 was separated from solution by neutralizing pH solution and centrifuging for 10 minutes. Finally, the as-synthesized MCM-41 was dried at 100 °C overnight and the organic template was removed by calcination at 540 °C for 6 hours to obtain MCM-41.

2-40%TiO_2/MCM-41s was synthesized with the similar method except that an appropriate amount TBOT was added into the milky sol-gel. TiO_2 was also synthesized with the same method as TiO_2/MCM-41s without addition of the rice husk silica.

3. Characterization of Catalysts

The phase of MCM-41, TiO_2 and TiO_2/MCM-41 was studied by X-ray diffraction (XRD: Bruker axs D5005 diffractometer) with Cu K_α radiation. Fine catalyst-powder (0.20 g) was pressed in a sample holder and scanned from 1.5 to 80 degree (2θ) with step size of 0.05 degree/minute. The diffraction patterns of the various powder samples were recorded with the same mass of the sample so that the diffraction intensity could be compared.

Physical characteristics including surface area and pore structure of the samples were determined from N_2 adsorption-desorption isotherm obtained at −196 °C in the relative pressure ranging from 0.01 to 0.99 with an Autosorb 1 MP (Quantachrome). Before the measurement, each sample was degassed at 80 °C for 4 hours. The BET surface area was obtained from the N_2 adsorption data in the relative pressure range of 0.02 to 0.2. The pore diameter was calculated from the adsorption-desorption branch that hysteresis was observed according to Barrett-Joyner-Halenda (BJH) method.

Morphologies of TiO_2, MCM-41 and TiO_2/MCM-41 powders were investigated with a transmission electron microscope (TEM JSM 6400). Specimens were dispersed in absolute ethanol, sonicated to disperse particles and deposited on a carbon-holey grid and dried in air. The specimens were scanned by TEM and recorded with various magnifications.

The change of band-gap energy was analyzed by diffuse reflectance UV-vis (DR UV-vis). All sample powders were homogeneously diluted with KBr in a mass ratio of 1 : 10. A mixture was compressed to 2,000 psi and measured by UV-Vis Lambda 650 model (Perkin Elmer) to determine UV absorption spectra in the range of 200-800 nm.

The electrophoretic mobilities of bare TiO_2, MCM-41 and TiO_2/MCM-41 particles were measured in aqueous suspension (1.0 g/L) to determine their zeta potentials as a function of pH by using an electrophoretic light scattering spectrophotometer (Zetasizer Nano ZS, Malvern) equipped with an He-Ne laser and a thermostatted flat board cell at the pH solution of 1 to 9.

4. Analysis of Chemical Composition in *E. camaldulensis* Leaves

To determine chemical compositions, fallen leaves of *E. camaldulensis* were extracted by water and organic solvents including hexane, dichloromethane, ethyl acetate and diethyl ether and analyzed extracted samples with HPLC HP 1100 Model (Agilent) equipped with a 1024-diode detector.

5. PCD of Gallic Acid

All experiments were performed in a Pyrex reactor (60 mL) with a silica window. An Hg-arc lamp (400 W) was used as the light source. All TiO_2, MCM-41 and TiO_2/MCM-41 suspensions were prepared at a concentration of 0.17-0.77 g/L, dispersed by simultaneous sonication and shaken for 30 seconds. An aliquot of gallic acid stock solution (1 mM) was subsequently added to the suspension to give the desired concentration. The initial pH (pH_i) of the suspension was adjusted with HCl or NaOH standard solutions. The suspension was stirred in the dark for 30 minutes and subsequently irradiated by UV light. The sample aliquots of 1 mL were collected at appropriate time intervals and filtered through 0.45-μm PTFE filters (Millipore). The concentration of gallic acid and its degradation products was analyzed by a HPLC hpv-1 (Shimadzu) equipped with a diode-array conductivity detector.

RESULTS AND DISCUSSION

1. Characterization

1-1. XRD

XRD of MCM-41 and anatase TiO_2 on MCM-41 are shown in Fig. 1(a)-(b). The major reflection of (100) pattern at the 2θ of 2.50° (Fig. 1(a)) belonged to characteristics of MCM-41, but two minor reflections of (110) and (210) patterns were not clearly observed at the 2θ between 4.05° and 4.69°. The intensity of the major reflection of (100) pattern decreased with amount of TiO_2 added, due to partially covering a part of the pore structure with TiO_2 [13]. The space of planes (d) calculated from the relationship: $d=(\sqrt{3}/2)a$ also

Table 1. Surface area of catalysts and textural properties of mesoporous materials

Materials	Surface (m^2/g)	a	d_{100}
MCM-41	1,059.9	43.8	37.9
5% TiO_2/MCM-41	720.0	43.2	37.4
10% TiO_2/MCM-41	695.5	42.6	36.9
20% TiO_2/MCM-41	556.9	41.0	35.5
40% TiO_2/MCM-41	532.9	39.3	34.0

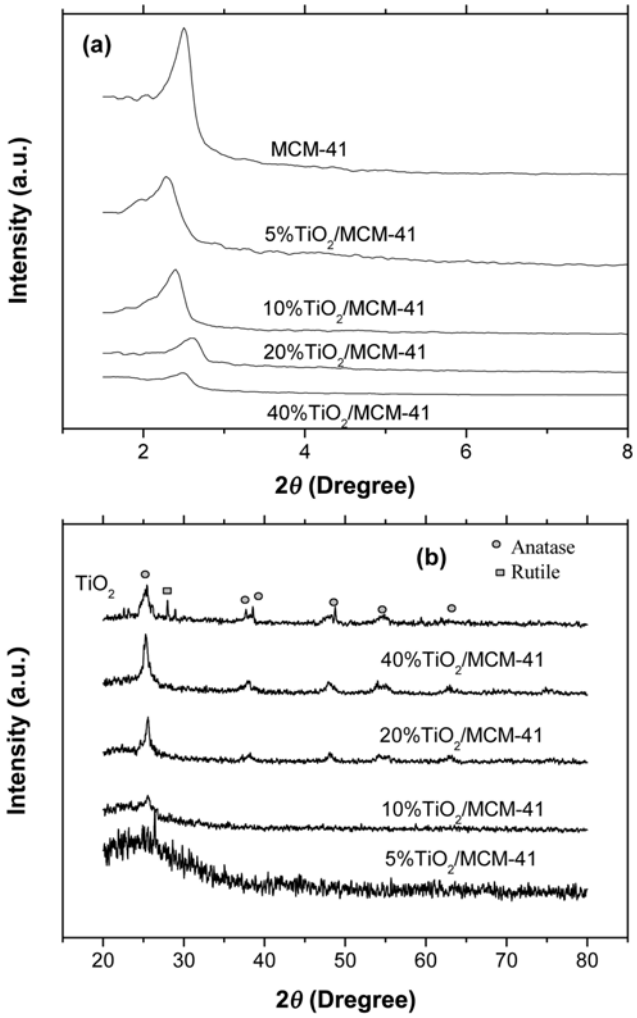

Fig. 1. XRD patterns: (a) MCM-41 and TiO_2/MCM-41 (b) Anatase and Rutile TiO_2.

decreased with loading of TiO_2, where a stands for the width of hexagonal arrays in MCM-41. Corresponding to the result of a previous investigation, Artkla et al. [11] have shown that a and d of MCM-41 obviously shifted to a lower 2θ due to incoming of TiO_2. All textural properties are shown in Table 1.

Fig. 1(b) manifested a high angel reflection of XRD patterns of TiO_2 and TiO_2/MCM-41s. The results showed that bare TiO_2 is composed of mixed phases of anatase and rutile at the 2θ between 24 and 65°. The anatase fraction was larger than the rutile. Reflection pattern of anatase majored at the 2θ of 25.4°, while one of rutile revealed at the 2θ of 27.9°. TiO_2/MCM-41 synthesized from pre-

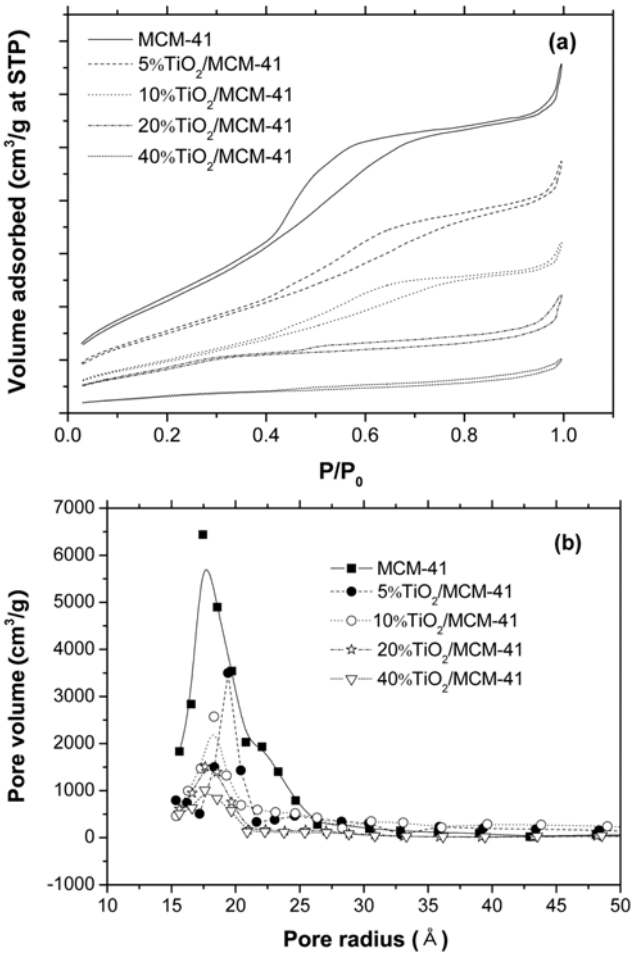

Fig. 2. (a) N_2 adsorption-desorption isotherm and (b) Pore size distribution of mesoporous materials.

impregnation possessed only anatase. The tendency increased along with the added amount of TiO_2. The anatase TiO_2 was described as active species for photodegradation of organic substances [14].

1-2. Nitrogen Adsorption-desorption

Nitrogen adsorption-desorption on TiO_2/MCM-41 as a relationship between relative pressure (P/P_0) and volume adsorbed at STP is shown in Fig. 2(a). The results show that the adsorption isotherms of MCM-41 and TiO_2/MCM-41 were type IV, which is characteristic of mesoporous materials. The adsorption at relative pressure around 0.0-0.2 was concave to the P/P_0 axis due to monolayer adsorption in external surface which were large pores. The lower adsorption volume on TiO_2/RH-MCM-41 indicated the lower surface area corresponding to the decrease of (100) diffraction planes of MCM-41 in the presence of TiO_2. A sharp inflection at relative pressure of 0.2-0.4 specified capillary condensation within uniformly sized mesopores. The hysteresis loop at the relative pressure greater than 0.4 revealed a secondary mesoporous system. A loop at relative pressure greater than 0.8 could be ascribed to condensation between small particles [15].

Specific surface areas of all catalysts are listed in Table 1. The surface area of TiO_2/MCM-41 decreased with the TiO_2 loading, indicating that TiO_2 partially sheltered some part of the surface area of MCM-41 [13]. Furthermore, the pore diameter of TiO_2/MCM-41

calculated from BJH equation was in the range of 15-30 Å, entailing regularity of pore size distribution, and possessed identical physical activity for catalysis of reaction [16]. However, the volume adsorbed of TiO_2/MCM-41s was greater than that of TiO_2, which demonstrated that the amount of adsorbed gallic acid on TiO_2/MCM-41s was greater that on TiO_2. Meanwhile, activities of all catalysts were expected to depend on adsorptive properties between reagent and active site (See Fig. 2(b)).

1-3. TEM

Analysis of internal structure of MCM-41 and TiO_2/MCM-41 with a TEM is demonstrated in Fig. 3(a)-(d). The results presented the hexagonal honeycomb of MCM-41 regularly rearranged in two dimensions as shown in Fig. 3(a). Fig. 3(b) illustrates the agglomeration of TiO_2 supported on mesopores of MCM-41. In this view, most of TiO_2 particles were well distributed across the hexagonal array of MCM-41 (Fig. 3(c)-(d)), confirming the regularity of the internal structure of catalysts and registering a good aspect of prepared catalysts for PCD.

1-4. DR UV-Vis

The width of the energy-gap between valence and conduction band is shown in Fig. 4. The band gap of TiO_2 was approximately 394.1 nm. With the amount of TiO_2 anchored into MCM-41, the band gap of 20%TiO_2/MCM-41 and 40%TiO_2/MCM-41 shifted to 402.5 and 425.1 nm, respectively, indicating that a chemical bond between TiO_2 and MCM-41 occurred and increased quantum efficiency to excite to the surface of catalyst, causing active species of hydroxyl radical ($HO^{\bullet}$) for PCD [17]. Due to the small loading of TiO_2 in 5%TiO_2/MCM-41 and 10%TiO_2/MCM-41, a band gap was not observed in this investigation.

1-5. Zeta Potential

The electrokinetic potential (zeta potential) at the surface of MCM-41 and TiO_2/MCM-41 is shown in Fig. 5. pH-dependence zeta potential of MCM-41, 10%TiO_2/MCM-41, 20%TiO_2/MCM-41, 40%TiO_2/MCM-41 and TiO_2 increased in the order of 2.11, 2.67, 3.20, 4.00 and 6.00 mV, respectively, corresponding to the results of Vohra et al. [10] and Artkla et al. [11]; the zeta potential of TiO_2/MCM-41s increased with TiO_2 loading. These electric voltages were related to pH zeta point of zero charge (pH_{PZC}), the pH of the solution that particles provide the ability to protect themselves from precipitation. In fact, TiO_2 precipitates at pH_{PZC} of 6-7, and this circumstance usu-

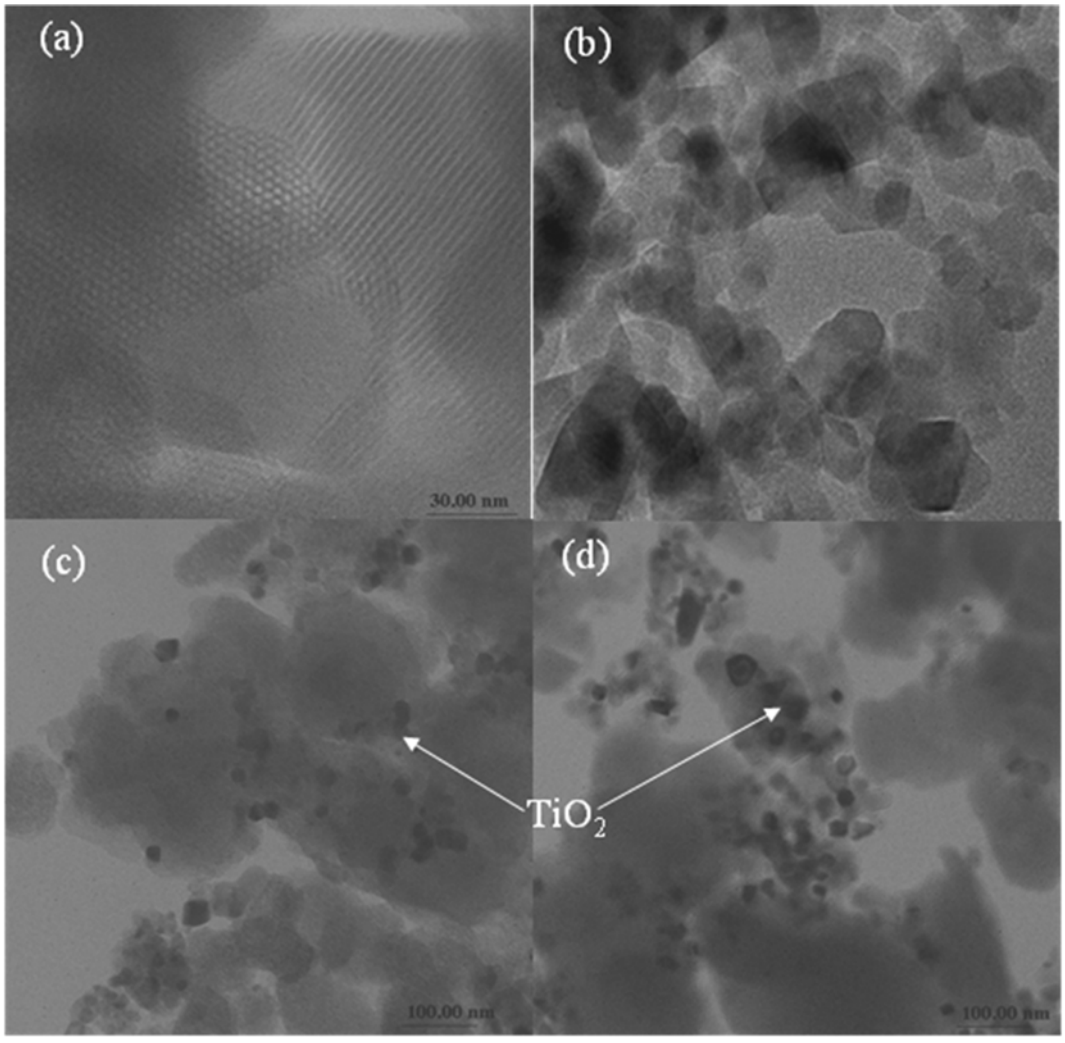

Fig. 3. TEM mesoporous materials (a) Hexagonal array of MCM-41 (100k), (b) Anatase TiO_2 (25k), (c) 10%TiO_2/MCM-41 (25k) and (d) 20%TiO_2/MCM-41 TiO_2 (25k).

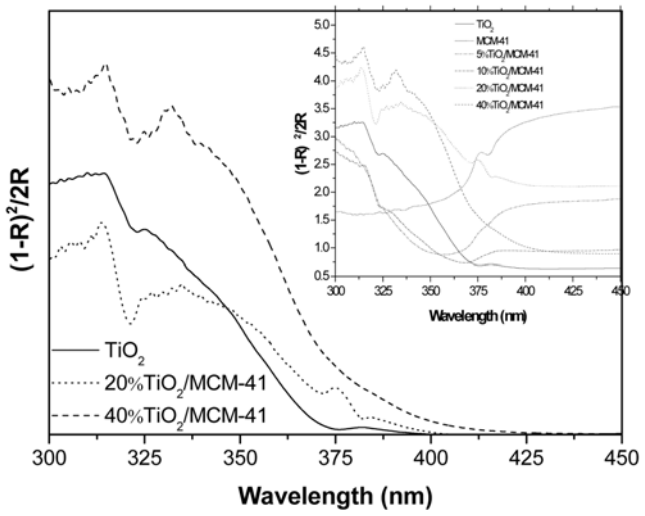

Fig. 4. DRUV-*Vis* of MCM-41 and TiO_2/MCM-41.

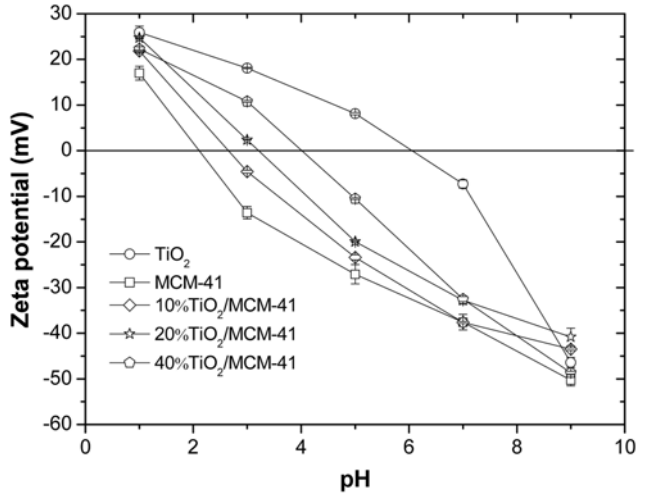

Fig. 5. Zetapotential of MCM-41 and TiO_2/MCM-41s.

Table 2. Chemical composition in *E. camaldulensis* leaves

Extracts of	Composition (mg/L)		
E. camaldulensis leaves	Flavone	Gallic acid	Tannic acid
Hexane	2.03	N/D	N/D
Diethyl ether	N/D	4.33	N/D
Ethyl acetate	7.32	8.16	N/D
Dichloromethane	6.05	N/D	N/D
Distill water	N/D	27.35	N/D

ally appears for accumulation of toxic matter in water. Bare TiO_2, hence, deactivates and does not practically work for PCD of sanitary water. Addition of MCM-41 in this experiment was expected to be a support for TiO_2 and facilitated the PCD of gallic acid.

2. Chemical Analysis of *E. camaldulensis* Leaves

The chemical analysis of *E. camaldulensis* leaves with HPLC is shown in Table 2. Chemical compositions dissolved in both organic solvents and distilled water. Of all chemicals in *E. camaldulensis* leaves, gallic acid was considered to be the most toxic (LD_{50}=5 mg/Kg) and preferred to solute in distilled water. It was found in this experiment that 27 ppm of gallic acid was extracted to distilled water. Consequently, gallic acid tended to degrade with UV light in the presence of TiO_2 and TiO_2/MCM-41s.

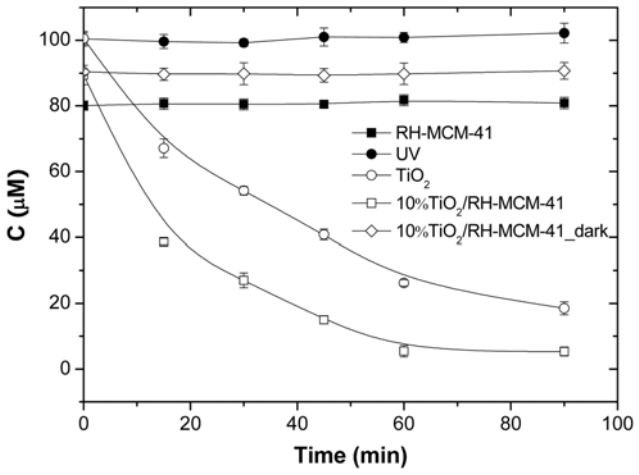

Fig. 6. PCD of catalysts; [TiO_2/MCM-41]=0.17 g/L, [TiO_2]=0.017 g/L, [gallic acid]=100 μM, pH=9.0.

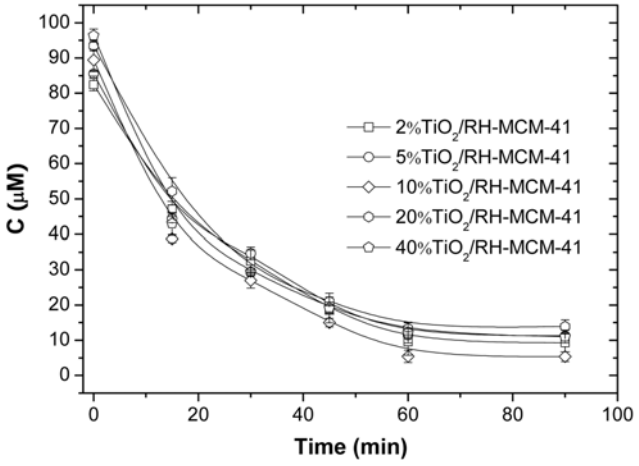

Fig. 7. Effect of TiO_2 loading to PCD of gallic acid; [TiO_2/MCM-41]=0.17 g/L, [gallic acid]=100 μM, pH=9.0.

3. PCD of Gallic Acid

3-1. Catalytic Activity

Fig. 6 shows the variation in PCD activities of gallic acid on all MCM-41, TiO_2 and TiO_2/MCM-41 irradiated with UV light. Utilization of a sole UV light could not degrade gallic acid in aqueous solution, whereas the reaction on pristine MCM-41 showed only 20% adsorption of gallic acid. The remaining gallic acid of 80 μM was observed after PCD was irradiated for more than 60 minutes. PCD was also neglected on all TiO_2/MCM-41s in the dark after reaching equilibrium at 30 minutes. Nevertheless, the adsorptive concentration of gallic acid had dramatically decreased due to partial vanishing of the catalytic surface area accompanied with TiO_2 loading. It was in turn found that PCD of gallic acid on 10%TiO_2/MCM-41 was obviously maximized and saturated after 60 minutes (see Fig. 7). The concentration of gallic acid, measured by HPLC, was under the detection limit, around 6 μM. Increasing TiO_2 loadings from 10

to 40% was not worthwhile because all reactions were as good as in PCD rate. In agreement with the previous study [11], the overloaded portion of TiO_2 greater than 10% on MCM-41 did not show an enhanced PCD. This was rationalized as that the synergistic effect of grafting TiO_2 on MCM-41 support might be saturated at 10% loading. On the other hand, PCD of gallic acid on bare TiO_2 synthesized in the same method was moderately lower than that on TiO_2/MCM-41. The concentration of 21 μM was still detected over the same time. This indicated that MCM-41 did not only act as a support but facilitated synergistic acceleration of PCD [18]. Corresponding to the result of Vohra et al. [10], PCD of TMA cation was greatly enhanced when adding silica as a support because of the denseness in OH functional groups on the surface. In addition, Hoffmann et al. [19] also described the availability of surface OH groups as being subscriptable in the ease of electrons to catalytic surface and generated a large number of activated •OH. Carp et al. [17] disclosed that the surface OH groups governed in adsorption of surrounding substrates around TiO_2 particles and facilitated PCD of ones with the UV light. From this point of view, MCM-41 which was polymerized chains of silicate groups (initiated from silica sources) accompanied with 10% of TiO_2 was believed to enhance PCP rate of gallic acid.

3-2. Effect of the Catalyst

The amount of 10%TiO_2/MCM-41 was systematically varied from 0.17 g/L to 0.77 g/L in aqueous solution of 100 μM gallic acid shown in Fig. 8. PCD of gallic acid was good for all concentrations. Increasing the amount of TiO_2/MCM-41 only extended adsorbed content of substrate not PCD rate-dependence. The adsorbed content of gallic acid increased from 5-10 wt% when the content of TiO_2/MCM-41 was further added from 0.17 g/L to 0.77 g/L. PCD activity was not significantly different with catalyst content. This point of view can be described in several reasons. First, adding large numbers of TiO_2/MCM-41 nanoparticles might cause fully screening UV light and cannot generate •OH, which is an active species for PCD [20]. Second, the catalytic activity of the TiO_2/MCM-41 was deactivated with excess content, probably due to collisions in the ground state of the catalyst [21]. Finally, TiO_2 nanoparticles in the solution not only screened the penetration of UV light to generate •OH but also scattered the UV light. Accordingly, the photoenergy of the UV light dropped and TiO_2 nanoparticles might deactivate by agglomeration in aqueous solution [22]. Thus, the concentration of 0.17 g/L of TiO_2/MCM-41 was used throughout the rest of the investigation.

3-3. Kinetics of the Reaction

PCD tendency of gallic acid on 10%TiO_2/MCM-41 in the presence of UV light revealed the linear regression in the relationship between $-\ln(C/C_0)$ and **t** with the R^2>0.95 and slope=−0.04255. The PCD of gallic acid obeyed pseudo-first order with a half-life of 1.6270 minutes (Fig. 9).

3-4. Effect of pH

PCD of organic substrates involves electron transfer from valence to conduction band to establish •OH. Catalytic surface charge also plays an important role in electron transfer and hole suppression and strongly depends on pH change [17]. As the previous statement, PCD of TMA cation was optimized for negatively charged surface of TiO_2/MCM-41. Gallic acid as a neutralized molecule in the normal aqueous solution (pH=6.5-7) was required to form the

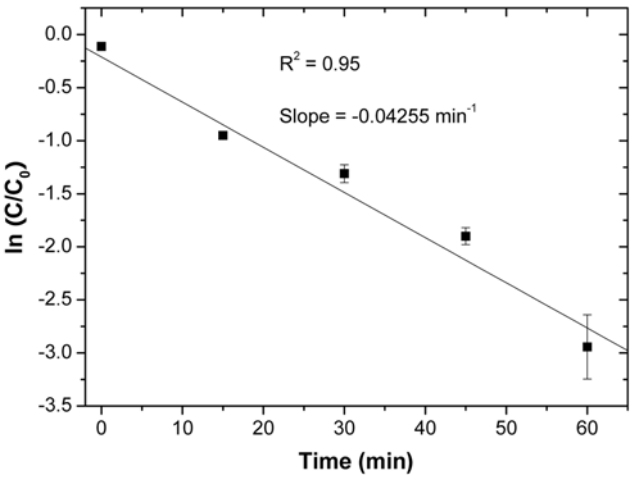

Fig. 9. Kinetics model of gallic acid degradation on 10% TiO_2/MCM-41; [TiO_2/MCM-41]=0.17 g/L, [gallic acid]=100 μM, pH=9.0.

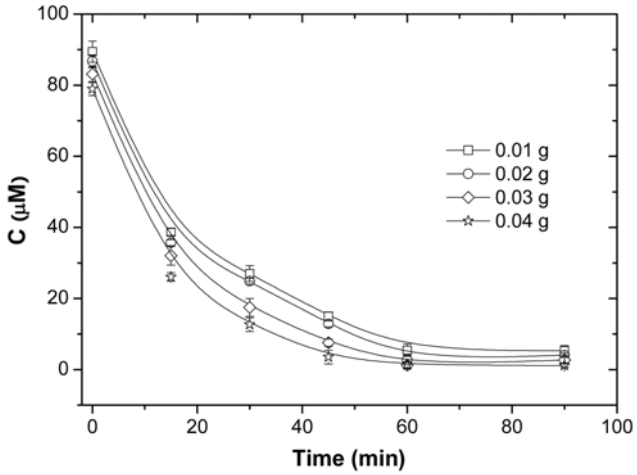

Fig. 8. Effect of catalyst content to PCD; Catalyst=10% TiO_2/MCM-41, [gallic acid]=100 μM, pH=9.0.

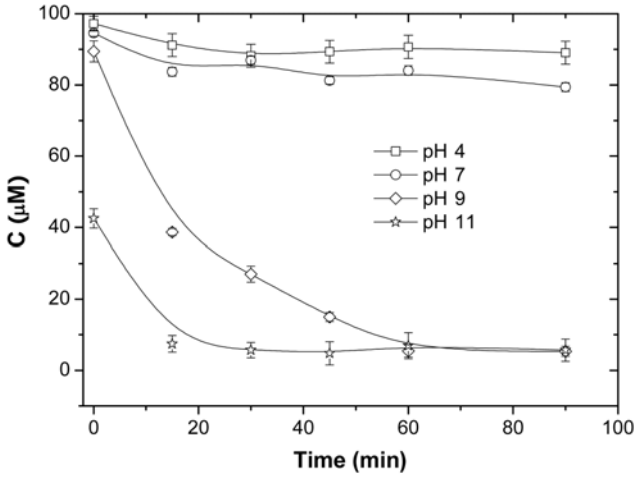

Fig. 10. pH dependence of PDC of gallic acid; [TiO_2/MCM-41]= 0.17 g/L, [gallic acid]=100 μM, pH=9.0.

positive charge with external auxiliaries. Thus, it is worth to consider the changes of both catalytic surface and the molecular charge against the pH changes.

The electrokinetic potential on the surface change of catalysts in this investigation was determined by adjusting pH point of zero charge (pH_{PZC}) in the pH range of 1 to 9. Taking into account the results from Fig. 10, at the pH solution in the range 4.25 to 7 ($7 \geq pH_{PZC} \geq 4.25$), gallic molecules ($pK_{a1}=4.0$) were still keeping neutral [23] and the interaction with negatively charged surface of 10%TiO_2/MCM-41 was minimized. Kim and Choi [9] confirmed that photogeneration of $^{\bullet}OH$ radical under this reduced condition was an obstacle at a pH solution below pH_{PZC}. PCD rate of positive ion (TMA) would not be considerably promoted. Like the reaction in positive ion, neutral molecule (gallic acid) would not form a positively charged complex by hydrogen bonding with H_2O at $pH<pKa_2$ (8.7) [23]. In accordance, the concentration of gallic acid was still greater than 80 μM after 60 minutes of irradiation. A small rate in the degradation was rationalized from several reports [9,11] that few $^{\bullet}OH$s had been established in the acidic aqueous solution and working pH solution was lower than pH_{PZC} of 10%TiO_2/MCM-41 (2.7). On the other hand, the adsorption at the pH solution over or equal to 9 ($pH_{PZC} \geq 9$) was optimized. Gallic acid was adsorbed for 10 wt% and degradation rate was highly enhanced until reaching the saturation at 6.03 μM of concentration. The optimal was reasoned as that gallic molecules were able to be deprotonized and bound hydrogen bonds with water [23]. Consequently, the negatively charged surface of 10%TiO_2/MCM-41 was able to form Coulomb interaction with positively charged H on gallic molecules. This implied that optimum charged interaction facilitated $^{\bullet}OH$ establishment after being accelerated with UV light, resulting in a considerable degradation of gallic acid [23, 24]. Nevertheless, it was a wonder that the increase pH solution over 10 did not enhance the PCD rate of gallic acid. Even though a considerable amount (42.45 μM) of gallic acid was adsorbed on 10%TiO_2/MCM-41, the PCD rate was still tenuous. It thus should be explained that the PCD activity of 10%TiO_2/MCM-41 was deactivated due to the internal mesopore collapses of MCM-41 at a pH solution higher than 10 [25,26]. In addition, Kim and Choi [27] declared that a large number of OH^- in the alkali solution might reveal Columbic repulsion to $^{\bullet}OH$ and sequentially suppress the $^{\bullet}OH$ establishment.

3-5. Possible Products from PCD of Gallic Acid

PCD degradation of gallic acid played a role by $HO_2^{\bullet}$, $O_2^{\bullet-}$ and $HO^{\bullet}$ which were generated from the separation of electron-hole from the band gap of TiO_2 [9,17]. Herein, the hydroxyl surface of MCM-41 also participated in trapping photogenerated holes that may cause electron-hole recombination and reduce photocatalytic efficiency of TiO_2/MCM-41 [19,28]. The generated reactive radicals then broke down the aromatic ring of gallic acid via intermediate pathway of formic acid, oxalic acid, pyruvic acid, malanic acid and maleic acids [29]. These intermediate carboxylic acids would be continuously trapped by hydroxyl surface in the vicinity of TiO_2 prior to mineralization of all generated intermediates to CO_2 and H_2O [28,30,31].

CONCLUSIONS

PCD of gallic acid on anatase TiO_2 could be enhanced by impregnating on MCM-41. The presence of anatase TiO_2 caused a decrease in the support surface area due to partial pore blocking, but the morphology and crystallinity did not change. Band gap energy of TiO_2 was bathochromic shift facilitating electron excitation. Gallic acid adsorption on TiO_2/MCM-41 (hybrid catalyst) was much higher than that on TiO_2. A significant improvement in the photocatalytic activity was obtained with 10 wt% of TiO_2 loading. The optimum concentration of hybrid catalyst with a fixed %TiO_2 loading was 0.17 g/L, whereas the increase %TiO_2 loading on the support with a fixed mass of the hybrid catalyst did not enhance the PCD activity. The PCD activity of 10%TiO_2/MCM-41 strongly depended on the solution pH and was maximal around the pH solution of 9 with the optimal charge interaction between gallic acid and TiO_2/MCM-41. A complete photocatalytic conversion of gallic acid was achieved in 60 minutes of irradiation. PCD with TiO_2/MCM-41 was faster in removal for 30 minutes. Kinetics of the reaction obeyed pseudo-first order. PCD of gallic acid was through the carboxylic intermediates which mineralized to CO_2 and H_2O.

ACKNOWLEDGEMENTS

S. Artkla appreciates the financial subsidy from the Office of the National Research Council of Thailand (NRCT), the Thailand Research Fund (TRF) and Roi-Et Rajabhat University (RERU), Thailand. Instrument support is from Scientific Equipment Center, Suranaree University of Technology, Nakhon Ratchasima, 30000, Thailand, and Research Laboratory Equipment Center, Maha Sarakham University, Maha Sarakham, 44000, Thailand.

REFERENCES

1. L. Bravo, *Nutr. Rev.*, **56**, 317 (1998).
2. R. Ahmed, A. T. M. R. Hoque and M. K. Hossain, *J. Forest Res.*, **19**, 19 (2008).
3. P. C. Gehrke, M. B. Revell and A. W. Philbey, *J. Fish Biol.*, **43**, 265 (1993).
4. M. Abelho and M. A. S. Graça, *Hydrobiologia*, **324**, 195 (1996).
5. A. Molina, M. J. Reigosa and A. Carballeira, *J. Chem. Ecol.*, **17**, 147 (1991).
6. S. Azabou, W. Najjar, A. Gargoubi, A. Ghorbel and S. Sayadi, *Appl. Catal. B: Environ.*, **77**, 166 (2007).
7. R. Capasso, A. Evidente, L. Schivo, G. Orru, M. A. Marcialis and G. Cristinzio, *J. Appl. Bacter.*, **79**, 393 (1995).
8. R. Borja, J. Alba and C. J. Banks, *Process Boichem.*, **32**, 121 (1997).
9. S. Kim and W. Choi, *Environ. Sci. Technol.*, **36**, 2019 (2002).
10. M. S. Vohra, J. Lee and W. Choi, *J. Appl. Electrochem.*, **35**, 757 (2005).
11. S. Artkla, W. Kim, W. Choi and J. Wittayakun, *Appl. Catal. B: Environ.*, **91**, 157 (2009).
12. S. Artkla, K. Wantala, B.-O. Srinameb, N. Grisdanurak, W. Klysubun and J. Wittayakun, *Korean J. Chem. Eng.*, **26**, 1556 (2009).
13. S. Artkla, W. Choi and J. Wittayakun, *Adv. Mater. Res.*, **93**, 22 (2010).
14. M. A. Zanjanchi, H. Golmojdeh and M. Arvand, *J. Hazard. Mater.*, **169**, 233 (2009).
15. G. A. Eimer, S. G. Casuscelli, G. E. Ghione, M. E. Crivello and E. Herrero, *Appl. Catal. A: Gen.*, **298**, 232 (2006).
16. M. V. Landau, L. Vradman, X. G. Wang and L. Titelman, *Micropor. Mesopor. Mater.*, **78**, 117 (2005).

17. O. Carp, C. L. Huisman and A. Reller, *Prog. Solid State Chem*., **32**, 33 (2004).
18. S. Artkla, W. Choi and J. Wittayakun, *Environment Asia*, **2**, 41 (2009).
19. M. R. Hoffmann, S. T. Martin, W. Choi and D. W. Bahnemann, *Chem. Rev.*, **95**, 69 (1995).
20. I. K. Konstantinou and T. A. Albanis, *Appl. Catal. B: Environ*., **49**, 1 (2004).
21. B. Neppolian, H. C. Choi, S. Sakthivel, B. Arabindoo and V. Murugesan, *Chemosphere*, **46**, 1173 (2002).
22. J. X. Mai, W. L. Sun, L. Xiong, Y. Liu and J. R. Ni, *Chemosphere*, **73**, 600 (2008).
23. A. C. Eslami, W. Pasanphan, B. A. Wagner and G R. Buettner, *Chem. Cent. J*., **4**, 15 (2010).
24. S. Kim and W. Choi, *J. Phy. Chem: B*, **109**, 5143 (2005).
25. N. Nishiyama, H. Saputra, D. H. Park, Y. Egashira and K. Ueyamaet, *J. Membr. Sci.*, **218**, 165 (2003).
26. D.-H. Park, H. Saputra, N. Nishiyama, Y. Egashira and K. Ueyamaet, *J. Chem. Eng. Jpn.*, **34**, 1321 (2001).
27. S. Kim and W. Choi, *Environ. Sci. Technol*., **36**, 2019 (2002).
28. A. Maira, K. L. Yeung, C. Y. Yan, P. L. Yue and C. K. Chan, *J. Catal*., **192**, 185 (2000).
29. F. J. Beltrá, O. Gimeno, F. J. Rivas and M. Carbajo, *J. Chem. Technol. Biotechnol.*, **81**, 1787 (2006).
30. J.-C. Lee, M.-S. Kim, C. K. Kim, C.-H. Chung, S. M. Cho, G. Y. Han, K. J. Yoon and B.-W. Kim, *Korean J. Chem. Eng*., **20**, 862 (2003).
31. H.-J. Lee, D.-W. Kang, J. Chi and D. H. Lee, *Korean J. Chem. Eng*., **20**, 503 (2003).